

# Preliminary Investigation of Iron Protoporphyrin SAMs on Platinum Electrodes by Surface Enhanced Vibrational Spectroscopies

MA Min, YANG Yao-yue, ZHANG Han-xuan, CAI Wen-bin \*

(Department of Chemistry, Fudan University, Shanghai Key Laboratory for Molecular Catalysis and Innovative Materials, Shanghai 200433, China)

**Abstract:** *In situ* SERS and ATR-SEIRAS were applied to investigate the electrochemical and structural properties of iron protoporphyrin IX (FePP) self-assembled monolayers (SAMs) on Pt electrodes in 0.1 mol · L<sup>-1</sup> HClO<sub>4</sub>. The potential dependent SERS spectra of the FePP SAM on a roughened Pt electrode with the enhancement factor of ca. 40 were acquired with the excitation line of 514 nm. Analyses of SERS data over the potential region from 0.5 to -0.3 V enabled to obtain potential dependent adsorption isotherms, from which the formal redox potential could be estimated to be ca. -0.2 V. Up-tilted orientation of FePP SAM on Pt film electrode involving one peripheral propionate group attached to the surface and one propionic acid group hydrogen-bonded with adjacent FePP, was deduced based on *in situ* ATR-SEIRAS results, without significant structural change over the potential region from -0.1 to 0.9 V.

**Key words:** SERS; SEIRAS; iron protoporphyrin IX; SAM; Pt electrodes

**CLC Number:** O646

**Document Code:** A

## Introduction

Surface-enhanced vibrational spectroscopies can provide valuable structural information of adsorbates on electrode surfaces. In the past two decades, the instrumental advancement of Raman spectrometers, the improved surface-roughening, and the delicate design of core-shell nanostructures have enabled to extend the application of electrochemical surface-enhanced Raman spectroscopy (SERS) from traditional coinage metals to Pt-group and iron-triad metals<sup>[1]</sup>. Meanwhile, the new development of facile chemical and electrochemical depositions of various metallic films on Si windows has also made it possible to expand the scope of interfacial phenomena as probed by *in situ* surface-enhanced IR absorption spectroscopy (SEIRAS)<sup>[2]</sup>.

Irreversibly adsorbed layers, mostly alkanethiol

self-assembled monolayers (SAMs) on gold and silver surfaces have been intensively studied by surface-enhanced vibrational spectroscopies<sup>[3]</sup>. Recently, new focus of study has been directed on these SAMs on Pt-group and Fe triad metal surfaces due to their potential applications in manipulating corrosive and catalytic properties of the underlying metals<sup>[4-6]</sup>. Metalloporphyrin molecules can also form SAMs on metals, among them, iron protoporphyrin IX (simplified as FePP hereafter) has attracted an intensive interest due to its important role in biologically mimetic and electrocatalytic reactions. In fact, SERS<sup>[7-8]</sup> and ATR-SEIRAS<sup>[9-10]</sup> have been used to investigate the redox behavior of FePP SAMs on Ag<sup>[7-8]</sup>, as well as the adsorbing of CO and NO ligands to FePP SAMs on Au<sup>[9-10]</sup>. While SERS is suitable for detecting the skeletal vibrations of FePP SAMs, SEIRAS is useful

for detecting polar ligands and peripheral groups of FePP SAMs.

In order to further extend these two vibrational spectroscopies to non-traditional SAMs-modified electrodes, in the present work, we preliminarily report the electrochemical and structural information for FePP SAMs on Pt electrodes as revealed with *in situ* SERS and ATR-SEIRAS.

## 1 Experimental

SERS-activation of a Pt electrode was realized with the so-called square-wave oxidation reduction cycles in  $0.5 \text{ mol} \cdot \text{L}^{-1} \text{H}_2\text{SO}_4$  according to a previous report<sup>[11]</sup>. The self-assembly of iron (III) protoporphyrin IX ( $\text{Fe}^{\text{III}}\text{PP}$ ) (Aldrich Chemical Co.) adlayers was achieved by immersing the SERS-active roughened Pt electrode in  $50 \mu\text{mol} \cdot \text{L}^{-1} \text{Fe}^{\text{III}}\text{PP}$ -containing  $0.1 \text{ mol} \cdot \text{L}^{-1}$  borax solution overnight. Raman spectra were taken on a confocal Raman microscope system (LabRam II, HORIBA Jobin Yvon) equipped with a 514 nm  $\text{Ar}^+$  laser and an air-cooled CCD detector. The microscope attachment was based on an Olympus BX40 system with a long working-distance (8 mm) lens ( $50 \times$ ) objective. The laser beam impinged on the surface at an incident angle of ca.  $90^\circ$  and the scattered light was collected by the microscope in the  $180^\circ$  backscattering geometry. A 1800-grooves/mm grating, a slit width of  $200 \mu\text{m}$  and a pinhole of  $600 \mu\text{m}$  were selected, yielding a spectral band pass of approximately  $2 \sim 4 \text{ cm}^{-1}$ . The radiation power on the electrode surface was about  $1.5 \text{ mW}$ , and the total acquisition time for each spectrum was 300 s.

The SEIRA-active Pt electrode was prepared according to the so-called two-step wet process in which a 60-nm-thick Au underfilm was first chemically deposited on the reflecting plane of a hemicylindrical Si prism followed by an electrodeposition of a pinhole-free 6-nm-thick Pt overfilm<sup>[2]</sup>. *In situ* ATR-SEIRA spectra were obtained by using Magna-IR E. S. P. System 760 FT-IR (Nicolet) with an unpolarized infrared radiation at an incidence angle of  $65^\circ$  with a spectral resolution of  $4 \text{ cm}^{-1}$ . All the spectra were

shown in the absorbance unit defined as  $-\log(I/I^0)$ , where  $I$  and  $I^0$  represent the sample (with FePP SAMs) and reference (without FePP SAMs) single-beam spectra at the corresponding potentials, respectively. Spectral analysis was carried out with the Grams 32 software package (Galactic, Inc).

Potential control was achieved with a ZF-3 potentiostat (Fangzheng Instruments, Shanghai) or a CHI660B electrochemistry workstation (CH Instruments, Shanghai). A platinum sheet and a saturated calomel electrode (SCE) were used as the counter and the reference electrodes, respectively. All the measurements were run at room temperature. The potentials reported here are quoted with respect to SCE.

## 2 Results and Discussion

Fig. 1 shows the cyclic voltammograms of a roughened Pt electrode before (solid line) and after (dotted line) FePP SAMs modification in  $0.1 \text{ mol} \cdot \text{L}^{-1} \text{HClO}_4$  within the hydrogen adsorption and desorption potential window. It could be seen that the presence of  $\text{Fe}^{\text{III}}\text{PP}$  SAMs decreased the surface Pt sites available for H electrosorption.

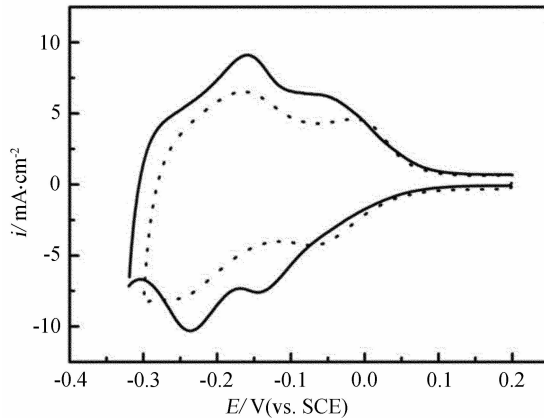


Fig. 1 Cyclic voltammograms for a Pt electrode before (solid line) and after (dotted line) being modified with FePP SAMs in  $0.1 \text{ mol} \cdot \text{L}^{-1} \text{HClO}_4$  at  $100 \text{ mV} \cdot \text{s}^{-1}$

Fig. 2 shows series of potential dependent SERS spectra for FePP SAMs on Pt electrode in  $0.1 \text{ mol} \cdot \text{L}^{-1} \text{HClO}_4$ , collected stepwisely from  $0.5$  to  $-0.3 \text{ V}$ , the corresponding band assignments are listed in Tab. 1. The bands at  $1566 (v_2)$ ,  $1487 (v_3)$  and  $1624$

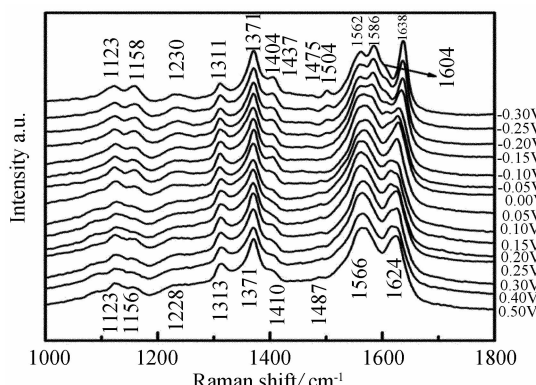


Fig. 2 Potential dependent SERS spectra of FePP SAMs on Pt electrode in  $0.1 \text{ mol} \cdot \text{L}^{-1}$   $\text{HClO}_4$  with  $514 \text{ nm}$  excitation line, acquisition time:  $300 \text{ s}$

$\text{cm}^{-1}$  ( $v_{10}$ ) at  $0.5 \text{ V}$  are characteristic of  $\mu$ -oxo form of  $\text{Fe}^{\text{III}}$  PP<sup>[7]</sup>. During the negative going potential movement to  $-0.3 \text{ V}$ , the  $v_2$ ,  $v_3$  and  $v_{10}$  bands shifted to  $1562$ ,  $1504$  and  $1638 \text{ cm}^{-1}$ , respectively, indicative of a decrease in the core size of the porphyrin skeletal ring, probably due to the potential induced transformation of the high-spin five-coordinated  $\text{Fe}(\text{III})$  state to the intermediate-spin four-coordinated  $\text{Fe}(\text{II})$  state<sup>[7]</sup>. It was reported that lowering solution pH to 3

caused the collapse of dimeric  $\mu$ -oxo  $\text{Fe}^{\text{III}}$  PP to monomeric  $\text{Fe}^{\text{III}}$  PP on Au and Ag electrodes<sup>[7]</sup>, however, here the dimeric  $\mu$ -oxo  $\text{Fe}^{\text{III}}$  PP appeared rather stable on the Pt electrode even at pH 1 at relative positive potentials. Specifically, the  $1487 \text{ cm}^{-1}$  feature kept largely unchanged from  $0.5 \text{ V}$  to  $0.05 \text{ V}$ , whereas the monomeric  $\text{Fe}^{\text{II}}$  PP feature, i.e., the band at  $1504 \text{ cm}^{-1}$  showed up only at potentials more negative than  $0.05 \text{ V}$ .

Unlike on carbon electrode, no clearly discernable voltammetric features associated with changes in redox state could be observed for FePP SAMs on Pt electrode. The central metal oxidation-state marker, i.e., the  $v_3$  band at  $1504 \text{ cm}^{-1}$  for the reduced state ( $\text{Fe}^{\text{II}}$  PP) was taken to estimate the formal potential of the FePP on Ag at pH 3<sup>[7]</sup>, yielding a value of  $-0.23 \text{ V}$ . In addition, the band around  $1311 \text{ cm}^{-1}$  could be used to normalize the intensity variation due to the inhomogeneous SERS effect across the Pt surfaces. From the peak position of the derivative curve of the isotherm (approximately

Tab. 1 Peak frequencies ( $\text{cm}^{-1}$ ) and assignments for selected vibrations of iron protoporphyrins on Ag, Pt and in solution

modes	<sup>a</sup> $\mu$ -oxo-Hemin pH 9.8	<sup>b</sup> $\mu$ -oxo-Hemin $\text{CH}_2\text{Cl}_2$	<sup>c</sup> SERS Ag pH 3		SERS Pt pH 1	
			Fe(III)	Fe(II)	Fe(III)	Fe(II)
$v_{10}$	$B_{1g}(\text{Ca-Cm})$	1616	1622	1628	1640	1624
$v_{37}$	$E_{1u}(\text{Ch-Ch})$		1585	1586	1587	undetected
$v_2$	$A_{1g}(\text{Ch-Ch})$	1560	1568	1570	1565	1566
$v_3$	$A_{1g}(\text{Ca-Cm})$	1480	1489	undetected	1504	1487
$v_{20}$	$A_{2g}$					1504
$v_{29}$	$B_{2g}(\text{Ca-N})$				1407	1410
$v_4$	$A_{1g}(\text{Ca-N})$	1363	1371	1372	1372	1370
$v_{21}$	$A_{2g\delta}(\text{CH}_2)$	1300		1311	1311	1313
$v_{30}$	$A_{2g\delta}(\text{Ch-Ca})$	1158	1167	1168	1163	1156
$v_6 + v_8$	$A_{1g}$	1118		1128	1127	1123
						1123

a. Data obtained in our laboratory for  $50 \mu\text{mol} \cdot \text{L}^{-1}$  FePP dissolved in  $0.1 \text{ mol} \cdot \text{L}^{-1}$  borax solution. Excitation line  $514 \text{ nm}$ .

b. Data from Refs. [ Sanchez et al. J. Phys. Chem. 89, 763, (1985)].

c. Data from Refs. [ Cai et al. J. Electroanal. Chem. 524-525, 36, (2002)].

represented by the percentage plot of the Fe<sup>II</sup>PP spectral contribution as a function of potential) as shown in Figure 3, the formal potential was roughly determined to be ca. -0.20 V for FePP SAMs on Pt electrode in 0.1 mol · L<sup>-1</sup> HClO<sub>4</sub>.

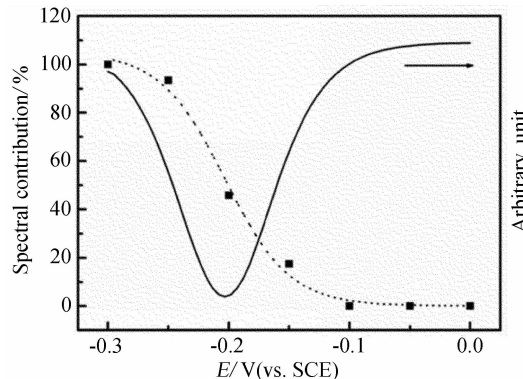


Fig. 3 Plots of the percentage of the spectral contribution of the 1504 cm<sup>-1</sup> band from Fe<sup>II</sup>PP as a function of potential

the peak-shaped curve represents the derivative of the adsorption isotherm (solid line) obtained from best fits to the experimental data(dashed line)

The surface enhancement factor is an important parameter for this type of functional electrode, which can be evaluated according to the formula below<sup>[12]</sup>:

$$G \approx \frac{hcN_A\sigma I_{surf}}{RI_{bulk}} = \frac{21cN_A\sigma I_{surf}}{RI_{bulk}} \quad (1)$$

where  $c$  is the bulk concentration of the analyte FePP in solution;  $N_A$  is the Avogadro's constant;  $\sigma$  is the surface area occupied by a unit of  $\mu$ -oxo Fe<sup>III</sup>PP (ca. 1.04 nm<sup>2</sup>)<sup>[13]</sup>,  $h$  is the height of waist of a focus laser beam in the bulk solution, which is about 21 μm for a pinhole size of 600 μm;  $R$  is the roughness factor of the Pt surface;  $I_{surf}$  and  $I_{bulk}$  is the integrated intensity of one vibrational band of FePP on Pt and in bulk solution, respectively. From Fig. 4, the ratio of the  $v_4$  band intensity for Fe<sup>III</sup>PP on Pt and in solution can be obtained, thus the surface enhancement factor of Fe<sup>III</sup>PP on Pt was estimated to be about 40. This low value seemed insufficient to yield good-quality surface Raman spectra, therefore, surface roughness factor and weak resonant Raman effect for FePP with the 514 nm excitation line should contribute to the much larger overall enhancement.

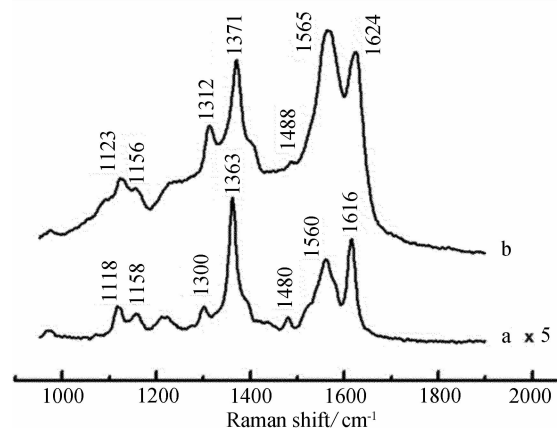


Fig. 4 Raman spectrum of 50 μmol · L<sup>-1</sup> FePP in 0.1 mol · L<sup>-1</sup> borax (a) and SERS of FePP on Pt in 0.1 mol · L<sup>-1</sup> HClO<sub>4</sub> (b) with an acquisition time of 300 s

In order to provide complementary structural information for FePP SAMs on Pt electrode, SEIRAS was also applied to determine the orientation of FePP SAMs on Pt electrode. Fig. 5 shows series of potential dependent SEIRAS of the FePP/Pt in 0.1 mol · L<sup>-1</sup> HClO<sub>4</sub>, collected stepwisely from 0.1 to 0.9 V with the reference spectra taken for the bare Pt electrode under otherwise same conditions. The peaks at 1716, 1388, 1438 and 1639 cm<sup>-1</sup> can be attributed to the C=O stretching vibration mode of hydrogen-bonded—COOH, the symmetric stretching mode of —COO<sup>-</sup>, the C—H deformation of short alkyl chains and the scissoring vibration mode of interfacial H<sub>2</sub>O<sup>[14]</sup>, respectively. The two peaks around 2900 cm<sup>-1</sup> are due to the CH<sub>2</sub> stretching modes. However, the antisymmetric stretching mode of the carboxylate group gave no resolved band that usually appeared in the 1500 ~ 1600 cm<sup>-1</sup> region, suggesting that the carboxylate group is bound to the Pt electrode in a symmetric geometry.

Different from FePP SAMs on Au electrode<sup>[9-10]</sup>, the frequencies and intensities for the δ<sub>co</sub> and ν<sub>oco</sub> bands were largely unchanged with the potential. The hydrogen-bonded —COOH of FePP may explain the rather stable adsorption over the potential range from 0.1 to 0.9 V. According to surface selection rule, the short CH<sub>2</sub> chain is tilted with respect to the metal surface, as evidenced by the appearance of CH stretch

bands in the  $3000 \sim 2800 \text{ cm}^{-1}$  region. Therefore, it may be proposed that the porphyrin plane is tilted to a local Pt surface with its peripheral propionate group attached to the surface through the bridge configuration, with its peripheral propionic acid group interacted with neighboring molecules through hydrogen bonding<sup>[14]</sup>.

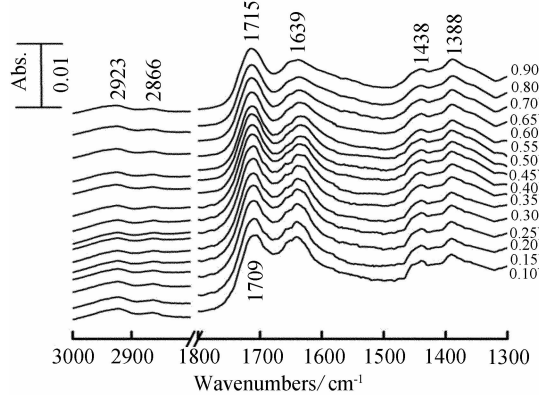


Fig. 5 Potential dependent ATR-SEIRA spectra for a FePP/Pt electrode in  $0.1 \text{ mol} \cdot \text{L}^{-1} \text{ HClO}_4$  (reference spectra and sample spectra were taken before and after FePP adsorption)

### 3 Conclusions

Electrochemical and structural properties of FePP SAMs on Pt electrodes in  $0.1 \text{ mol} \cdot \text{L}^{-1} \text{ HClO}_4$  have been initially investigated with *in situ* SERS and ATR-SEIRAS. Analyses of SERS spectral data, specifically, the potential dependent intensity variation of an oxidation state marker, or the  $v_3$  band, enabled the formal redox potential of FePP SAMs to be estimated to be ca.  $-0.2 \text{ V}$ . Up-tilted orientation of FePP on Pt electrode was assumed based on *in situ* ATR-SEIRAS data with a nearly unchanged configuration, involving one peripheral propionate group attached to the surface, and one propionic acid group hydrogen-bonded with other molecules.

### References :

- [1] Tian Z Q, Ren B, Wu D Y. Surface-enhanced Raman scattering: From noble to transition metals and from rough surfaces to ordered nanostructures [J]. The Journal of Physical Chemistry B, 2002, 106:9463-9483.
- [2] Yan Y G, Li Q X, Huo S J, et al. Ubiquitous strategy for probing ATR surface-enhanced infrared absorption at platinum group metal-electrolyte interfaces [J]. Journal of Physical Chemistry B, 2005, 109:7900-7906.
- [3] Ulman A. Formation and structure of self-assembled monolayers [J]. Chemical Reviews, 1996, 96:1533-1554.
- [4] Silien C, Dreesen L, Cecchet F, et al. Orientation and order of self-assembled p-benzenedithiol films on Pt(111) obtained by direct adsorption and via alkane-thiol displacement [J]. Journal of Physical Chemistry C, 2007, 111:6357-6364.
- [5] Hoertz P G, Niskala J R, Dai P, et al. Comprehensive investigation of self-assembled monolayer formation on ferromagnetic thin film surfaces [J]. Journal of the American Chemical Society, 2008, 130:9763-9772.
- [6] Wolpers M, Viehaus H, Stratmann M. Surface analytical investigations of metal-surfaces modified by Langmuir-Blodgett-Films of silanes [J]. Applied Surface Science, 1991, 47:49-62.
- [7] Cai W B, Stefan I C, Scherson D A. Determination of adsorption isotherm of species adsorbed on roughened silver electrodes from *in situ* quantitative surface enhanced Raman spectroscopy [J]. Journal of Electroanalytical Chemistry, 2002, 524:36-42.
- [8] Shi Q F, Cai W B, Scherson D A. In situ surface-enhanced Raman scattering studies of the nitrosyl adduct of hemin adsorbed on roughened silver surfaces in aqueous electrolytes [J]. Journal of Physical Chemistry B, 2004, 108:17281-17284.
- [9] Ma M, Yan Y G, Huo S J, et al. In situ surface-enhanced IR absorption spectroscopy on CO adducts of iron protoporphyrin IX self-assembled on a Au electrode [J]. Journal of Physical Chemistry B, 2006, 110: 14911-14915.
- [10] Ma M, Yan Y G, Wang J Y, et al. A study of NO adducts of iron protoporphyrin IX adlayer on au electrode with *in situ* ATR-FTIR spectroscopy [J]. Journal of Physical Chemistry C, 2007, 111:8649-8654.
- [11] Tian Z Q, Gao J S, Li X Q, et al. Can surface Raman spectroscopy be a general technique for surface science and electrochemistry? [J]. Journal of Raman Spectroscopy, 1998, 29:703-711.
- [12] Cai W B, Ren B, Li X Q, et al. Investigation of surface-enhanced Raman scattering from platinum electrodes using a confocal Raman microscope: dependence of surface roughening pretreatment [J]. Surface Science, 1998, 406, 9-22.

- [13] Bianco P, Haladjian J, Draoui K. Electrochemistry at a pyrolytic-graphite electrode—Study of the adsorption of hemin [J]. Journal of Electroanalytical Chemistry, 1990, 279: 305-314.
- [14] Zhang Z J, Imae T, Hydrogen-bonding stabilized self-assembled monolayer film of a functionalized diacid, protoporphyrin IX zinc (II), onto a gold surface [J]. Nano Letters, 2001, 1: 241-243.

## 铂电极上自组装铁原卟啉单分子层的表面增强 振动光谱初探

马 敏, 阳耀月, 张涵轩, 蔡文斌\*

(复旦大学化学系, 上海市分子催化和功能材料表面重点实验室, 上海 200433)

**摘要:** 应用现场表面增强拉曼光谱和衰减全反射表面增强红外光谱初步研究了  $0.1 \text{ mol} \cdot \text{L}^{-1}$   $\text{HClO}_4$  溶液中 Pt 电极表面铁原卟啉(FePP)自组装单层的电化学和结构特性。以 514 nm 波长为激发线, 得到了增强因子约为 40 的粗糙 Pt 电极上 FePP 在不同电位下的表面增强拉曼光谱。分析  $0.5 \sim -0.3 \text{ V}$  (SCE) 区间内谱峰变化, 得到近似的吸附等温式, 由此可估算出  $\text{Fe}^{3+}/\text{Fe}^{2+}$  的式量电位大约为  $-0.2 \text{ V}$ 。原位表面增强红外光谱的测试结果表明, FePP 分子主要以斜立方式吸附在 Pt 膜电极表面, 其中一个环外羧酸根与电极表面相接触, 而另一羧酸基团以氢键与相邻的 FePP 分子相连。这样的吸附结构在  $-0.1 \sim 0.9 \text{ V}$  (SCE) 的电位区间内并没有显著的变化。

**关键词:** 表面增强拉曼光谱; 表面增强红外光谱; 铁原卟啉; 自组装单分子层; 铂电极